# Intense field techniques for ultrafast quantum control of $D_2^+$

**C. R. Calvert, D. S. Murphy, J. McKenna, J. F. McCann and I. D. Williams**
*School of Mathematics and Physics, Queen's University Belfast, University Road, Belfast, BT7 1NN, UK*

**J. Wood, E. M. L. English and W. R. Newell**
*Department of Physics and Astronomy, University College London, Gower Street, London, WC1E 6BT, UK*

**W. A. Bryan**
*Department of Physics, Swansea University, Singleton Park, Swansea, SA2 8PP, UK*

**I. C. E. Turcu, S. J. Hawkes, J. M. Smith, E. J. Divall, K. G. Ertel, O. Chekhlov, C. J. Hooker, A. J. Langley and J. L. Collier**
*Central Laser Facility, STFC, Rutherford Appleton Laboratory, Chilton, Oxon, OX11 0QX, UK*

Main contact email address c.calvert@qub.ac.uk

## Introduction

The study of molecules in intense femtosecond laser pulses has been a research area attracting much interest in recent years. Fragmentation and ionization processes have been studied extensively, with recent studies achieving temporal resolution of the vibrational[1,2,3,4,5,6] and rotational[7,8] motion in the fastest molecular systems. Steps are now being taken towards ultrafast quantum control of molecules[9,10,11], with possible applications in quantum information studies[11,12]. An ideal system for such studies is the deuterium molecular ion, $D_2^+$. This system offers the theoretical tractability of the fundamental three-body molecule $H_2^+$, but its slower nuclear motion provides increased experimental accessibility for time resolved studies.

This brief report details two approaches for achieving quantum control of $D_2^+$. First, a technique is presented for controlling the nature of the photodissociation mechanism, i.e. whether the molecule dissociates via net absorption of one photon (1ω) or two photons (2ω). Control is experimentally demonstrated with theoretical simulations seen to be in good accord. Secondly, the simulations are extended to demonstrate the possibility of state selective control of the vibrational population in future experiments. The quantum simulations illustrate the possibility of cooling the nuclear wavepacket into a restricted subset of the lowest vibrational levels, with potential application in quantum encoding/information studies. With current advances in laser technology, such experiments may be realized in the near future.

## Controlling the dissociation pathway of $D_2^+$

A target $D_2^+$ ion may be created by field induced tunnel ionization of the neutral $D_2$ molecule and will remain bound for internuclear separation (R) ranging from ≈ 1 to 5 au, where the nuclear wavepacket dictates the probability density as a function of R (shown schematically in Figure 1). The interaction of a second pulse can then be used to probe the vibrational dynamics of the system via photodissociation, PD. This proceeds by net absorption of either one photon (1ω) or two photons (2ω) and separates the molecule into deuteron ($D^+$) and deuterium (D) fragments. This PD mechanism has been studied in detail and recently the temporal evolution of the dissociating molecule has been observed using the Astra laser[13,14] and elsewhere[15].

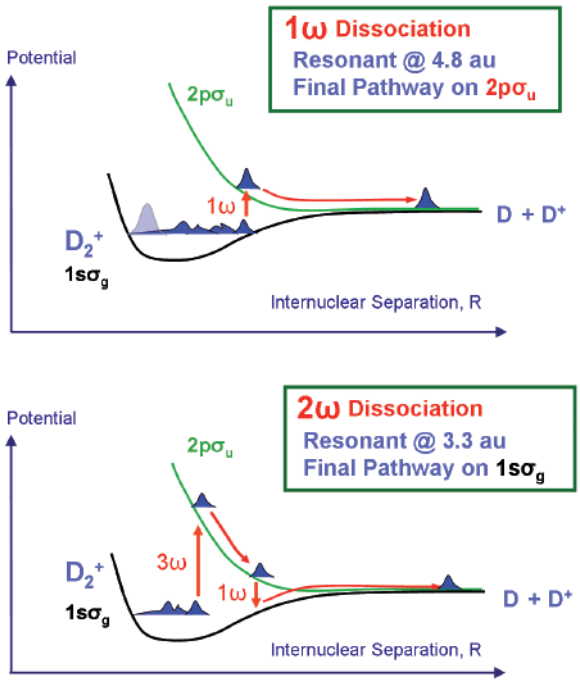


**Figure 1. Schematic of intense field processes in $D_2^+$. Upper diagram: Initial creation of $D_2^+$ target by tunnel ionisation gives the initial probability density at small R (schematic in light blue). The wavepacket may time evolve (dark blue) and subsequent irradiation of this target can give 1ω dissociation, projecting the bound wavepacket onto repulsive $2p\sigma_u$ state, or 2ω dissociation (lower diagram) with the dissociating wavepacket on the $1s\sigma_g$ state.**

The 1ω process occurs when the bound $D_2^+$ molecule (in the $1s\sigma_g$ electronic state) absorbs one photon, and the wavepacket is projected onto the repulsive $2p\sigma_u$ state, see upper diagram in Figure 1. Upon this repulsive curve, the nuclear wavepacket may escape to large R and, thereby, dissociate. For 790 nm light this process is resonant at R ≈ 4.8 au. However the bandwidth of the ultrashort laser pulse (upwards of 100 nm for the pulses considered here) leads to absorption and emission from either end of the spectral profile and introduces a spread of energies for the dissociating fragments. The lower diagram in Figure 1 shows that 2ω dissociation occurs via absorption of 3 photons (projection onto $2p\sigma_u$ curve) and subsequent emission of 1 photon (back onto $1s\sigma_g$). These transitions

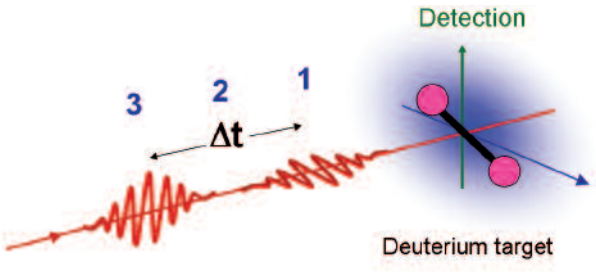


**Figure 2. The three steps to control of dissociation products from $D_2^+$. 1. Pump pulse to create $D_2^+$ ion. 2. The molecule vibrates for time Δt. 3. The probe pulse dissociates the molecule.**

are resonant around 3.3 au and 4.8 au respectively and the molecule gains enough energy from the dissociative motion between these R values to overcome the remaining barrier and dissociate along the $1s\sigma_g$ potential. Thus the 2ω dissociating wavepacket trajectory is along the $1s\sigma_g$ potential at large R, whereas the 1ω path is along $2p\sigma_u$. It is important to note that the 1ω and 2ω channels are enhanced at different internuclear separations, and are thus dependent on the position of the bound wavepacket when the laser pulse is applied.

The dynamics of the dissociation process can therefore be studied by using a simple pump probe technique with two ultrashort pulses, separated by a time delay, Δt (see Figure 2). The first pulse creates the coherent vibrating $D_2^+$ molecule. After time delay Δt the wavepacket has evolved to a particular distribution in R and is subsequently dissociated by the probe pulse, leading to 1ω or 2ω dissociation.

The results from an experimental study of this scheme are shown in Figure 3(a). This was carried out using ultrashort pulses from the Astra laser in TA1. 30 fs pulses from the Ti: Sapphire laser system were passed into a hollow fibre – chirped mirror compression system [16], and subsequently through a Mach Zehnder interferometer to provide on-target pulses of 14 fs duration. The temporal delay, Δt, was adjustable by means of a motorised translation stage which enabled the path length of the probe pulse to be varied in steps of 0.05μm, providing a temporal separation of 1/3 fs. These pump and probe pulses were aligned into a time of flight mass spectrometer (TOFMS) and reflection

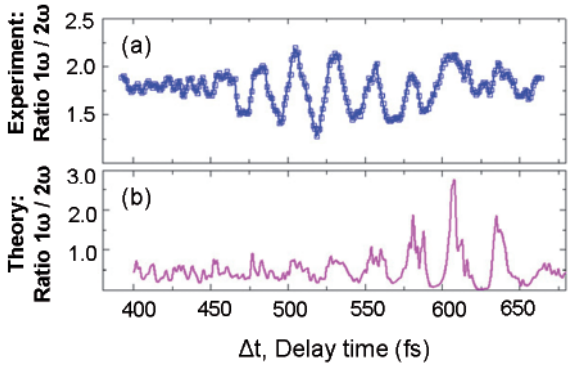


**Figure 3. Ratio of 1ω/2ω dissociation channels when the bound $D_2^+$ ion is probed at delay time Δt. (a) Experimental results. (b) 2-state simulation.**

focussed (f/5 spherical mirror) onto a $D_2$ gas target. The pump pulse polarisation was orientated perpendicular to the detection axis, ensuring that any dissociating fragments from the first pulse went undetected. The remaining bound wavepacket was then sampled by the probe pulse, with polarisation parallel to detection axis. Charged products (deuterons) from the interaction of the second pulse were extracted by a weak electric field (2000 V $cm^{-1}$) and collected at a micro channel plate detector with their flight times recorded via a fast digital storage oscilloscope. The fragmentation energies could be readily deduced from the flight times and, thus, for each Δt value an energy spectrum was obtained for the dissociating fragments.

Relative contributions from 1ω and 2ω channels were determined by Gaussian fitting to the spectra, with the low energy 1ω process centred around 0.39 eV and the higher energy 2ω process around 0.82 eV. Comparison of the areas under the 1ω and 2ω Gaussian fits thus provided a measure of 1ω/2ω ratio at each Δt value. This was carried out over a large range of Δt values, with the corresponding 1ω/2ω ratios shown in Figure 3(a). It is clear from the figure that the 1ω/2ω ratio displays notable modulation as a function of delay time and that the proportion of the wavepacket on each dissociative pathway can be controlled by this simple time-delay technique. The ratio displays a periodic structure of about 25 fs, due to the vibrational motion of the wavepacket [17].

Corresponding quantum simulations have also been carried out, with details of the calculation discussed elsewhere [10]. In brief, the nuclear wavepacket dynamics are simulated within a 1D wavepacket model, subject to the Born-Oppenheimer and two-state approximations. The bound $D_2^+$ wavepacket is initiated by projection of the $D_2$ (v=0) state onto the $D_2^+$ ($1s\sigma_g$) potential (Franck-Condon transition). The resulting temporal evolution of the coherent wavepacket is modelled by means of a Taylor propagator (up to 8th order). The wavepacket is allowed to evolve for a chosen delay time, Δt after which the probe pulse is applied. This applied pulse is modelled by a field of wavelength 790 nm (central λ) with a Gaussian profile, full width half max = 14 fs. The probe acts to couple the $1s\sigma_g$ state to the $2p\sigma_u$ state, resulting in wavepacket transfer in the presence of the intense-field pulse. After the pulse has elapsed, the theoretical treatment enables measurement of the $2p\sigma_u$ population at large R (1ω dissociation) and the $1s\sigma_g$ at both large R (2ω dissociation) and small R (bound wavepacket). Thus for each Δt value the resulting 1ω/2ω ratio can be estimated from the wavepacket simulation, as shown in Figure 3 (a).

There is good agreement with the experimental data for the periodicity of the Δt-dependent modulation of the 1ω/2ω ratio. For example, at around 555 fs, 580 fs and 605 fs 1ω dissociation is seen to dominate. However for shorter delay times (< 450 fs) the 2ω process is predicted by theory to be dominant in contradiction to the experimental observation. This discrepancy can however be attributed to the fact that the theoretical model does not include the competing Coulomb explosion fragmentation channel. Nonetheless, the simulation confirms the experimental observation that the 1ω/2ω ratio (and thus energies of dissociation products) can be controlled by temporally selective, ultrafast probing. Hence, the theoretical treatment employed here may be

regarded as an appropriate representation of the molecular system in such ultrashort intense fields and may be used to prompt future experimental studies. The motion of this dynamic system is inherently dependent on the vibrational distribution and in the next section we consider how ultrashort pulses may be utilised to exert coherent control on the vibrational population.

## State selective control of a $D_2^+$ vibrational wavepacket

A $D_2^+$ ion created via intense-field-induced ionisation is known to exist in a distribution of different vibrational states. The exact vibrational distribution is dependent on pulse duration [18] but for few-cycle pulses of IR light (one cycle = 2.67 fs) appears to be Franck-Condon (FC) [1,2,10], with about the first 15 vibrational levels populated. The fact that an ensemble of molecules may be coherently ionized by ultrashort laser pulses means that the dynamic motion of the superposition of vibrational states may be readily studied.

The possibility of state selective vibrational control with ultrashort pulses then provides a means by which the wavepacket motion may be deterministically influenced. It has been shown previously [17] that, owing to the anharmonicity of the $1s\sigma_g$ potential, different vibrational eigenstates contributing to the coherent wavepacket rapidly dephase (and subsequently revive), with the quantum nature of these vibrations departing significantly from the classical picture. However, by restricting the vibrational population of the ion to a fewer number of states it may be possible to reduce or even remove such dephasing effects and moreover achieve a vibrational qubit vis-à-vis quantum information studies [11].

To this end, an experimental scheme [11] for state selective control of the $D_2^+$ vibrational wavepacket is proposed, using an ultrashort intermediate control pulse in between the pump and probe pulses. The quantum simulations described in the first section have been extended to study this scenario. A wavepacket initiated in a Franck Condon distribution is allowed to temporally evolve prior to application of a controlling pulse. Rather than measure the dissociation signal, it is possible to focus on the fraction of the nuclear wavepacket population that remains bound during application of the control pulse. In particular, the absolute population of the different vibrational levels can be extracted. The results from such a calculation are shown in Figure 4, for a control pulse ($2\times10^{14}$ Wcm$^{-2}$, 14 fs fwhm) applied at 20 fs. The pulse profile is shown in the upper panel (E-field in au). The lower panel displays the temporal evolution of the vibrational population, for the five lowest vibrational eigenstates.

Prior to the application of the control pulse, the populations of states v = 0 - 4 are displayed (given by the appropriate Franck Condon weightings). For the particular delay time illustrated, the control pulse shifts population, predominantly, into the two lowest vibrational levels (i.e. v = 0 and 1). Although some small residual population remains in higher-lying levels and dissociation will also have occurred for a portion of the wavepacket, the bound wavepacket motion is undoubtedly dictated by 0 and 1 levels after the application of control pulse at 20 fs.

This same technique can be applied across a range of control pulse delay times with the resulting vibrational

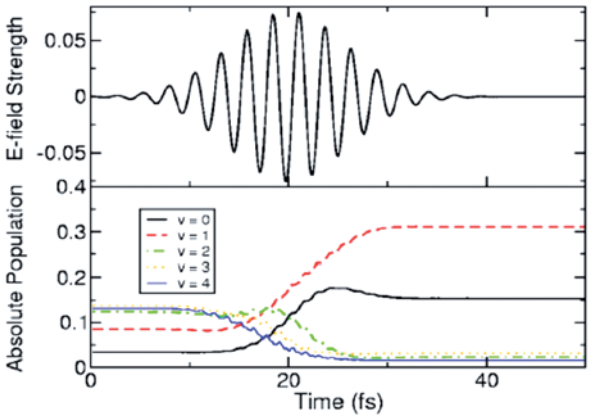


**Figure 4. State selective manipulation of vibrational population in $D_2^+$ (lower panel) by application of a 14 fs, $2\times10^{14}$ W cm$^{-2}$ IR control pulse (upper panel).**

distributions extracted in each case. Thus the final populations can be shown as a function of control pulse delay time, and this is illustrated in Figure 5. Here the control pulse parameters are the same as before and the four lowest vibrational levels are considered. Two particularly interesting points, A and B, are highlighted and correspond to resulting wavepackets in even superpositions of v = 0 and 1, and v = 1 and 2, respectively. The consequence of these distributions on the motion of the temporally evolving wavepacket is illustrated in Figure 6.

The plot in Figure 6(a) shows the field-free wavepacket motion of the coherent $D_2^+$ wavepacket in a Franck Condon distribution, as created by the pump pulse. This has been discussed in detail in previous reports [6, 17]. The wavepacket starts at small R values and initially moves back and forth across the potential (large R-amplitude) with all vibrational states in phase, however, these components quickly dephase and the motion starts to become averaged across the potential.

For a control pulse applied after an appropriate delay the resulting wavepacket motion differs dramatically from the field-free case, as seen in Figure 6 (b) and (c). The superposition of v = 0 and v = 1 states, arising from the control pulse applied at 18.7 fs, gives rise to wavepacket

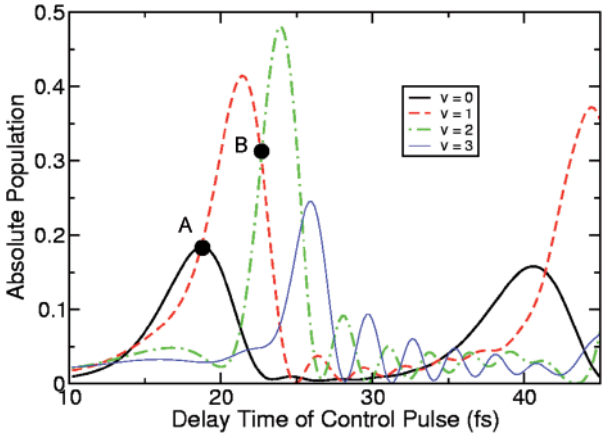


**Figure 5. Final vibrational distribution as a function of control pulse delay time. (Control pulse parameters as in Figure 4).**

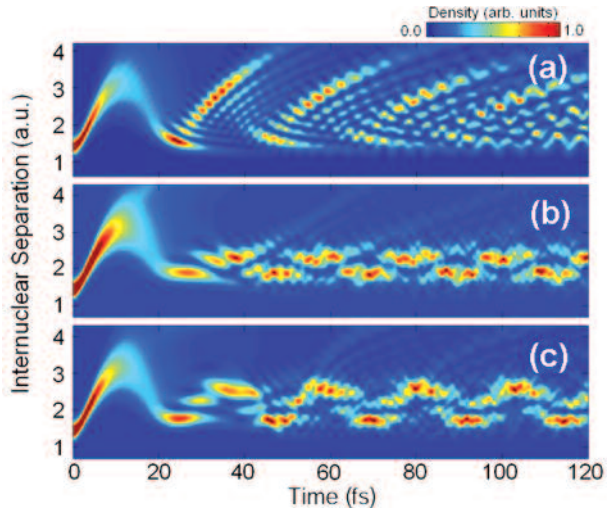


**Figure 6. Probability density of the vibrational wavepacket as a function of time. (a) No control pulse. (b) Control pulse at 18.7 fs. (c) Control at 22.7 fs. Vibrational cooling is evident in (b) and (c) where the wavepacket is restricted to small R values and possesses less vibrational energy than the field free case in (a).**

motion that is clearly restricted to small R values (1.5< R <2.7 au). Here the nuclear system has been cooled to the two lowest-lying vibrational states and the resulting wavepacket motion is effectively semi-classical, executing localized oscillations with a period of ≈ 24 fs. A similar effect can be seen for the 22.7 fs delay time, where a vibrationally cooled wavepacket is created in v = 1 and 2 states. These higher-lying vibrational levels give rise to oscillations over a slightly larger range of R values (up to 3 au). This form of vibrational cooling is distinctly different from dissociative cooling (loss of population from higher-lying states) because, as seen in Figure 4, the absolute populations of the low v states increase.

Previous considerations of ultrafast vibrational cooling have demonstrated a shift in vibrational population [9], and discussed this in terms of the modification of the potential surfaces via the laser-induced Stark effect. The cooling mechanism may alternatively be discussed in the context of transitions between the field-free potentials in the presence of the laser field [11]. Here the bound molecule, when moving inwards in R, is projected onto the repulsive $2p\sigma_u$ electronic state and loses kinetic energy before being projected back onto $1s\sigma_g$ state, now with less energy. Physically, this means that the electron distribution shifts from being concentrated between the deuteron nuclei ($1s\sigma_g$) to an electron cloud outside the nuclei (dissociative $2p\sigma_u$), effectively unshielding the nuclei and enhancing the Coulomb interaction between them. If this occurs when the bond is contracting, then the Coulomb force acts to decelerate the motion, leading to vibrational cooling. Concordantly, if the bond is expanding (R increasing) then the wavepacket may gain energy, and be vibrationally heated [11].

The possibility of cooling the molecular ion to a coherent superposition of two vibrational levels presents an ideal system for quantum manipulation studies. For example, the control pulse at 18.7 fs can be used to produce even weighting of v=0 and 1 states and further pulse operations can be exacted on the system. One possibility, discussed in detail elsewhere [11], is to use a second control pulse to transfer population between these states via Raman transitions. This approach takes advantage of the dynamic nature of the system whereby the delay time of the second control pulse enables selective operations for enhancing v=0 (at delay time 64 fs) or to enhance v=1 (at delay time 74 fs) population. With ongoing advances in laser technology, it is hoped that such quantum control may be demonstrated experimentally in the near future.

## References


1. J. McKenna *et al.*, *J Phys: Conf Ser.* **58**, 375 (2007).
2. J. McKenna *et al.*, *J. Mod. Opt* **54** Issue 7, 1127 (2007).
3. Th. Ergler *et al.*, *Phys. Rev. Lett.* **97**, 193001 (2006).
4. A. Rudenko *et al.*, *Chem. Phys.* **329**, p193-202 (2006).
5. Th. Ergler *et al.*, *Phys. Rev. Lett.* **97**, 103004 (2006).
6. J. Wood *et al.*, *CLF Annual Report* (2005-2006), p88-90.
7. W. A. Bryan *et al.*, accepted to *Phys. Rev. A.*
8. E. M. L. English *et al.*, *CLF Annual Report* (2005-2006), p77-79.
9. H. Niikura *et al.*, *Phys. Rev. Lett.* **92**, 133002 (2004).
10. D. S. Murphy *et al.*, *J. Phys. B.* **40**, S359-S372 (2007).
11. D. S. Murphy *et al.*, accepted to *New Journal of Physics* (2007).
12. W. A. Bryan *et al.*, in preparation.
13. C. R. Calvert *et al.*, *J Phys: Conf Ser.* **58**, 379 (2007).
14. C. R. Calvert *et al.*, *CLF Annual Report* (2005-2006), p74-76.
15. Th. Ergler *et al.*, *Phys. Rev. Lett.* **95**, 093001 (2005).
16. I. C. E. Turcu *et al.*, *CLF Annual Report* (2004-2005), p223-225.
17. J. McKenna *et al.*, *CLF Annual Report* (2005-2006), p84-87.
18. X. Urbain *et al.*, *Phys. Rev. Lett.* **92**, 163004 (2004).
19. C. P. Hauri *et al.*, *Appl. Phys. B.* **79**, 673-677 (2004).
20. H. Niikura *et al.*, *Phys. Rev. A.* **73**, 021402 (2006).